

Observational Black Hole Spectroscopy: A time-domain multimode analysis of GW150914

Gregorio Carullo,^{1,2} Walter Del Pozzo,^{1,2} and John Veitch³

¹*Dipartimento di Fisica “Enrico Fermi”, Università di Pisa, Pisa I-56127, Italy*

²*INFN sezione di Pisa, Pisa I-56127, Italy*

³*Institute for Gravitational Research, University of Glasgow, Glasgow, G12 8QQ, United Kingdom*

(Dated: April 15, 2022)

The detection of the least damped quasi-normal mode from the remnant of the gravitational wave event GW150914 realised the long sought possibility to observationally study the properties of quasi-stationary black hole spacetimes through gravitational waves. Past literature has extensively explored this possibility and the emerging field has been named “black hole spectroscopy”. In this study, we present results regarding the ringdown spectrum of GW150914, obtained by application of Bayesian inference to identify and characterise the ringdown modes. We employ a novel pure time-domain analysis method which infers directly from the data the time of transition between the non-linear and quasi-linear regime of the post-merger emission in concert with all other parameters characterising the source. We find that the data provides no evidence for the presence of more than one quasi-normal mode. However, from the central frequency and damping time posteriors alone, no unambiguous identification of a single mode is possible. More in-depth analysis adopting a ringdown model based on results in perturbation theory over the Kerr metric, confirms that the data do not provide enough evidence to discriminate among an $l = 2$ and the $l = 3$ subset of modes. Our work provides the first comprehensive agnostic framework to observationally investigate astrophysical black holes’ ringdown spectra.

Introduction—GW150914 [1], being the first and loudest BBH detected so far, provided evidence for the presence of a ringdown phase at the end of the coalescence process. The ringdown spectrum, a superposition of quasi-normal modes (QNMs) and late-time power-law tails [2–5], directly ties to fundamental properties of the underlying spacetime. As a consequence of the final state conjecture (i.e. no-hair theorems plus the conjecture that the Kerr solution is a dynamical attractor for BH spacetimes in astrophysical scenarios) [6–15] the physical spectrum of QNMs is exclusively determined by the asymptotic BH mass and spin, hence ringdown observations of astrophysical BHs have the potential of verifying the Kerr nature of these objects. Moreover, an accurate determination of the BH ringdown spectrum represents, at the moment, one of the most promising avenues to unveil BH horizon quantum effects, discovering exotic compact objects, hairy BHs or even wormholes [16–18]. Several authors proposed methods and offered predictions on the feasibility of what has come to be known as “black hole spectroscopy” [19–22].

The first determination of a compact object QNM by the LIGO and Virgo Collaborations (LVC) [23–25] revealed the intrinsic difficulties in determining the transition between the non-linear merger regime to the quasi-linear one, where the results of BH perturbation theory are applicable [26]. Several studies based on numerical relativity simulations [27, 28], have proposed a fixed start time of $\sim 15M$ after the peak strain of the waveform. However, to validate these claims and to perform theory-agnostic measurements of the BH spectrum, we require the ability to measure the start time directly from the

data. With this, we can robustly test the remarkable predictions of GR, such as the black hole area increase law [29].

In this *letter*, we present the first comprehensive spectroscopic analysis of the GW150914 ringdown signal that, by operating directly in time domain, successfully identifies from the data the time of transition and identifies the most probable subset of QNM in the data. This is achieved employing a generic damped sinusoids ringdown model which does not include GR predictions on its complex frequencies, thus is generic enough to incorporate the emission of alternative compact objects possibly mimicking ringdown signals. We find no evidence in support of the presence of a second mode in addition to the one already identified in the LVC analysis. The central frequency and decay time measured with the generic model indicate that the most-probable modes can be *a posteriori* identified with a subset of the $\ell = 2$ and $\ell = 3$ modes as predicted by a Kerr solution [30]. We further refine our results by adopting a more informed model based on the theoretical spectrum of a Kerr BH. We demonstrate, in agreement with the generic approach, that the $(3, -3, 0)$, $(3, -2, 0)$, $(2, 1, 0)$ and $(2, 2, 0)$ modes are consistent with the remnant mass and spin of GW150914. The transition time estimate is consistent with the result obtained with the previous model. Unless explicitly noted, all statistical bounds reported are 90% credible regions.

Time domain analysis—Inference of the properties of the remnant BH is critically dependent on the ability to separate the quasi-linear regime, where perturbation theory is valid, from the non-linear merger regime [22, 26, 28, 29]. We perform our analysis in the time domain and

use data from the two Advanced LIGO detectors, provided by the Gravitational-Wave Open Science Center [31, 32]. We model the detector noise as a wide-sense stationary Gaussian process, hence fully described by its 2-point autocovariance function $C(\tau)$:

$$C(\tau) = \int dt n(t) n(t + \tau), \quad (1)$$

which we estimate from 4096 s of data surrounding the event. The 4096 s of data sampled at a rate of 4096 Hz are first band-passed with a 4th order Butterworth filter in the band [20, 2028] Hz. They are subsequently split into \mathcal{X} second long chunks and the autocovariance is computed

$$\log p(d|\theta, I) = -\frac{1}{2} \int \int dt d\tau (d(t) - h(t; \theta)) C^{-1}(\tau) (d(t + \tau) - h(t + \tau; \theta)),$$

where the domain of integration extends over the considered segment of data. The time-domain implementation of the likelihood solves several technical issues of the analysis, providing a convenient framework to avoid Gibbs phenomena arising from the FFT of a fast-rising template which can pollute the analysis of the BH spectrum. The analysis was performed using **CPNest**, an efficient python parallel nested sampling algorithm [33].

Agnostic analysis – We begin by attempting to infer the central frequency and damping time, and thus attempt to identify the mode, from the GW150914 ringdown signal. Hence, we relax as many assumptions as possible and assume a model defined by an *agnostic* superposition of damped sinusoids:

$$h_+ - ih_\times = \sum_i \mathcal{A}_i e^{i\tilde{\omega}_i(t-t_i) + \phi_i}. \quad (2)$$

where $\tilde{\omega}_i \equiv \omega_i + i/\tau_i$ is the complex ringdown frequency. The set $\{\omega_i, \tau_i, \phi_i, \mathcal{A}_i, t_i\}_{i \in \mathcal{N}}$ is treated as a set of free and independent parameters to be estimated from the data. The sum runs over the index i which serves as a label for the \mathcal{N} modes considered. Thus, we do not explicitly consider the frequency and damping times dependence on the mass and spin of the remnant black hole. In addition to the frequency and damping time, we consider also the ringdown amplitudes \mathcal{A}_i and start times t_i as parameters to be inferred directly from the data.

The prior distribution on the intrinsic parameters was chosen to be uniform within the ranges: $f_i \in [100, 500]$ Hz, $\tau_i \in [0.5, 20]$ ms, $\log_{10} \mathcal{A}_i \in [-19, -23]$, $\varphi_i \in [0, 2\pi]$ rad, $t_i \in [3.3, 6.6]$ ms after the peak of the waveform. The prior on the start time corresponds to the specific choice of $[10, 20] M_f$ after the peak time of the strain (during the analysis $t = 1126259462.423$ s at LIGO Hanford site

as the mean of the individual autocovariances estimated on each chunk, excluding the one containing the time of the trigger to be analyzed. To validate our noise estimation method, we exploit the Wiener-Khinchin theorem and compare the Fourier transform of the obtained autocovariance with the power spectral density (PSD) of the noise, estimated employing the standard Welch method. We find that a good agreement between the two estimates is obtained by choosing $\mathcal{X} = 2$. We verified that any choice of $\mathcal{X} > 2$ does not affect our conclusions. The log-likelihood function for the observed strain series $d(t)$, given the presence of a GW signal $h(t)$ is thus:

was chosen, in agreement with Ref. [26]). This choice is guided by numerical relativity studies that explicitly looked at the beginning of the linearized ringdown regime validity [34]. Different choices on the prior on the start time will be systematically investigated in a future study. $M_f = 68 M_\odot$ (in geometric units) is the median value of the estimate presented in [35]. In addition to the intrinsic model parameters, we sample the sky position angles and polarisation, to obtain the detector strain:

$$h(t) = F_+(\alpha, \delta, \psi) h_+ + F_\times(\alpha, \delta, \psi) h_\times \quad (3)$$

where $F_+(\alpha, \delta, \psi)$, $F_\times(\alpha, \delta, \psi)$ are the detector angular response functions [36]. For all the models employed in this *letter*, we chose our prior distribution to be isotropic for the source's sky location, and uniform in the polarisation angle $\psi \in [0, \pi]$.

We start by analyzing the data assuming a single mode damped sinusoid model. This approach aims at detecting the most excited mode directly from the data, being agnostic to GR predictions. Fig. 1 shows the joint posterior distribution for the central frequency f and damping time τ from our analysis. We find $f = 234_{-12}^{+11}$ Hz and $\tau = 4.0_{-1.0}^{+1.5}$ ms, which is consistent both with the predicted values from a full Inspiral-Merger-Ringdown (IMR) analysis and with the late time ($t_{\text{start}} \geq t_{\text{merger}} + 3\text{ms}$) unmodelled analyses in Refs. [22, 26]. To investigate which mode has the highest probability of matching the recovered unmodelled posterior *a posteriori*, according to GR predictions, we use the samples for the progenitors masses and spins released by the LVC [37], combined with fitting formulae obtained from numerical relativity simulations [20, 38, 39] and employ them to *predict* the corresponding frequency and damping time for a set of modes which overlap with the unmodelled posterior. Figure 1 shows

the 90% CI on $n = 0, l = 2, 3$ modes obtained with the described procedure. The largest overlap, quantified through Bayes theorem, is obtained for the $\{(2, 2, 0), (3, -3, 0)\}$ modes. We also find $\mathcal{A} = (3.22^{+1.4}_{-1.1}) \times 10^{-21}$, and, most notably, for the first time we determine directly from the data $t_{\text{start}} = 3.9^{+0.3}_{-0.3}$ ms. The uncertainty on the t_{start} is mostly due to the 4096 Hz sampling rate used. This latter result will be consistent across every analysis we presented in this *letter*. Interestingly, if one assumes the mass of the remnant BH to be $M_f = 68 M_\odot$ (the median value published by the LVC [26]), this corresponds to a start time for the ringdown of $\sim 14^{+2}_{-2} M_f$. This result is in good agreement with the aforementioned numerical relativity studies and consistent with results obtained through gauge-invariant geometric and algebraic conditions quantifying local isometry to the Kerr spacetime [27] and results obtained through earlier parameter estimation methods [28]. It is interesting to notice that we also infer a posterior distribution on the sky position of the signal (and consequently the relative time delay) which overlaps with published LVC analyses using the full signal [37, 40]. However, due to the lower SNR contained in the ringdown-only portion of the signal, our posterior distribution is wider. Fig. 2 shows the reconstructed signal obtained by our analysis on top of interferometric data. A whitening procedure is applied in order to facilitate the visualization of the result, but no whitening is applied during the analysis.

At this point it is natural to ask whether the data provides evidence for a second ringdown mode. To verify this hypothesis we repeat the previous analysis using the aforementioned settings, but now using two independent damped sinusoids. The obtained logB is reported in Table I and shows no statistical evidence for more than a single mode. We also attempted a test of GR through the measurement of $\delta\omega$ following [41], but the obtained posterior was found to be uninformative, consistently with the fact that the SNR present in GW150914 does not allow to constrain more than a single mode. Finally, a preliminary study on numerical solutions of the Einstein equations showed no challenges in testing the no-hair conjecture in the high SNR limit, contrary to the claim presented in [42] and confirming the results presented in [22, 28, 43].

Single Kerr mode – From the spectroscopic analysis the favoured subset of modes turned out to be the $(3, -3, 0)$, $(3, -2, 0)$, $(2, 1, 0)$ and $(2, 2, 0)$. A clear mode identification would require the width of the agnostic posterior to overlap with only a single mode, but the statistical uncertainty does not allow for a clear single-mode identification. Physical arguments (together with numerical relativity simulations) suggest that in the region of the parameter space which contains GW150914 the $(2, 2, 0)$ mode should be the most excited one. Hence, we wondered whether a stronger assumption can help discriminate between the competing modes and whether it confirms or refutes the results

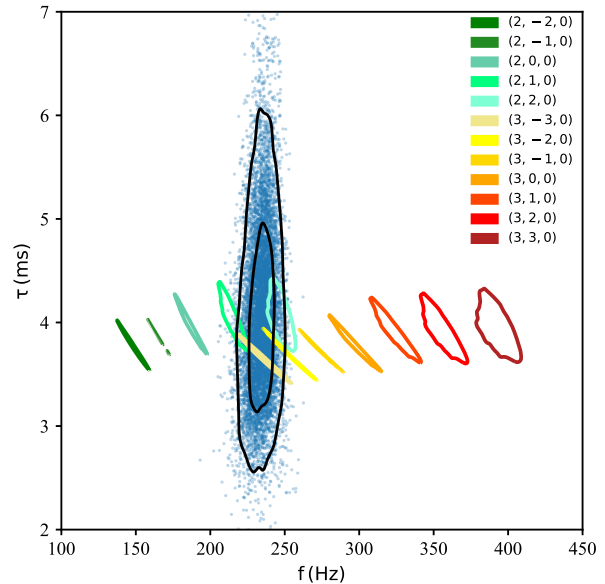


FIG. 1. BH spectroscopy from the two-dimensional posterior for central frequency and damping time obtained with a single damped sinusoid ringdown model. The colored contours are the 90% credible intervals for particular (ℓ, m, n) Kerr modes, derived from the LVC reported remnant mass M_f and spin a_f . We show the $\ell = 2$ and $\ell = 3$ modes as other ℓ 's do not overlap with the posterior distribution.

obtained with the unmodelled analysis. In order to do so, we run the analysis employing a Kerr model:

$$h_+ - ih_\times = \frac{M_f}{D_L} \sum_{lmn} \mathcal{A}_{lmn} S_{lmn}(\iota, \varphi) e^{i(t-t_{lmn})\tilde{\omega}_{lmn} + \phi_{lmn}}, \quad (4)$$

where again $\tilde{\omega}_{lmn} = \omega_{lmn} + i/\tau_{lmn}$ is the complex ringdown frequency. For the Kerr model, $\tilde{\omega}_{lmn}$ is determined by the remnant BH mass M_f and its spin a_f by relations $\omega_{lmn} = \omega_{lmn}(M_f, a_f)$, $\tau_{lmn} = \tau_{lmn}(M_f, a_f)$ that follow the formulae given in Ref. [20] and are also available at [39]. S_{lmn} are the spin-weighted spheroidal harmonics [44]. On the other hand, while analytic predictions for the amplitudes \mathcal{A}_{lmn} exist [34, 43, 45, 46] based on the progenitors masses and spins, we do not consider them in here, as our purpose is to agnostically estimate modes excitations, allowing observational comparisons to the aforementioned theoretical models. Finally, as in the previous analysis, the start time of each mode is left as a free parameter and determined by the analysis. The prior distribution was uniform within the ranges $D_L \in [10, 1000]$ Mpc, $\cos(\iota) \in [-1, 1]$, $M_f \in [10, 100] M_\odot$, $a_f \in [0, 0.99]$, $\log_{10} A_{lmn} \in [-5, 3]$, $\varphi_i \in [0, 2\pi]$ rad, $t_i \in [3.3, 6.6]$ ms.

In Table I we report, for the most probable modes, the Bayes factors comparing the hypotheses that GW150914 can be described as the ringdown generated by a single

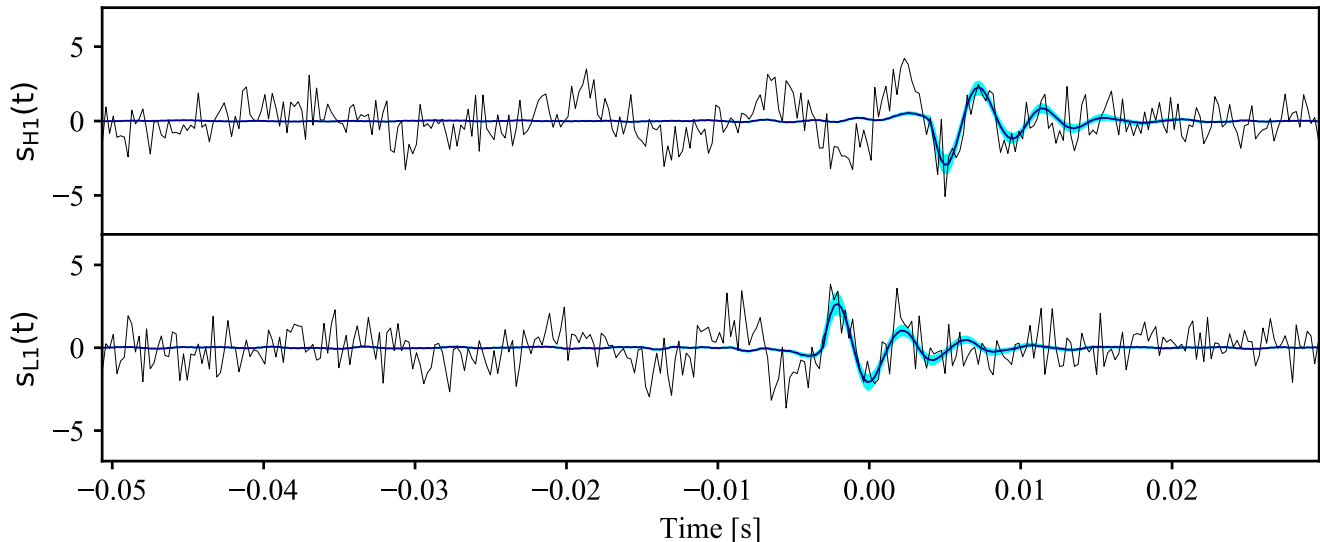


FIG. 2. Reconstructed whitened waveform superimposed on LIGO-Hanford (top panel) and LIGO-Livingston (bottom panel) data. The solid line shows the median recovered waveform, while shaded regions represent 90% credible intervals.

given (ℓ, m, n) Kerr mode. Without imposing any a priori restriction on the excitations of the different modes, the given SNR does not allow to conclusively discriminate between a subset of the $\ell = 2, 3$ modes.

Kerr multiple modes – Although the unmodelled analysis showed no evidence for more than one mode, a natural question is whether an analysis including more information (and less parameters to be sampled to avoid Occam razor’s related effects) can provide evidence for the presence of more than one mode in GW150914 late post-merger data. To tackle this question we repeat the analysis presented in the previous section, but now allowing two modes to vary at the same time. Several combinations were considered, in Table I we report a few of them which gave the higher Bayes factors. The results on the two Kerr parameters (mass and spin) of this analysis using the $\{(2, 2, 0), (3, -3, 0)\}$ modes is presented in Figure 3. We wish to stress that the posteriors therein do not imply the presence of multiple modes, but rather explain why the Bayes factors indicate that we cannot distinguish between a pure $(2, 2, 0)$, a pure $(3, -3, 0)$ or even a mixture of the two, see Table I. Both modes, in fact, provide similar predictions for central frequency and damping time for GW150914 – see also Fig. 1 – for the typical remnant parameters expected from near equal mass merging BH, where the resulting spin $a_f \sim 0.6$ is dominated by the contribution from the angular momentum of the orbit [47, 48]. From the spectral content only, the inability to discriminate among the $(2, 2, 0)$ and $(3, -3, 0)$ modes is thus likely to persist in future ground-based observations. We expect this degeneracy to be lifted either by very loud events or in systems for which the remnant spin is not dominated by the orbital angular momentum.

We also note that, regardless of the final state details, the best systems for spectroscopic studies will be the ones for which the orbital configuration is such that the dominant ringdown mode will be the $(2, -2, 0)$.

Up to now we kept a semi-phenomenological approach, but a more motivated choice of mode combination would be (for example) the use of all m modes for a given ℓ , e.g. for $\ell = 2$ $\{(2, 2, 0), (2, 1, 0), (2, 0, 0), (2, -1, 0), (2, -2, 0)\}$. This more generic model implies a much larger number of parameters to be sampled and, consequently looser bounds. Results for runs using all the $\ell = 2, 3$ modes are summarized in Table I and show no conclusive preference towards one specific ℓ . In all cases the sky position posterior distribution was found to be completely overlapping with the published LVC result, while orientation parameters (D_L, ι) cannot be well-estimated due to the complete degeneracy with mode amplitudes. The recovered posterior on start time shows minimal variations with respect to the one obtained by the damped-sinusoid analysis, for all the employed modes. Its stability with respect to the employed model is a strong indication of the stability of the method employed here, since no variation between different modes start times are expected to be detectable with the SNR contained in the post-merger portion of GW150914.

Summary and discussion – We presented the first comprehensive spectroscopy study on the GW150914 ringdown data. For the first time, we directly *measured* the ringdown onset time from the data, which was found to be consistent with predictions coming from fully non-linear solutions of Einstein’s equations. We confirm the presence of a ringdown signal with central frequency $f = 234^{+11}_{-12}$ Hz and damping time $\tau = 4.0^{+1.5}_{-1.0}$ ms, in agreement with pre-

TABLE I. Summary of the Bayes factors, M_f , a_f median (when measured) and 90% CI obtained with different waveform models and a transition time prior in [3.3, 6.6] ms. The statistical errors on the log Bayes' factors are ± 0.1 . They are estimated computing their variance over 10 different realisations of the pseudo-random number chain initialisation. Within the statistical errors, when differences of $\log B$ are compared against heuristic evidence scales, such as the Jeffreys scale, no significant evidence in favor of any specific mode (or combination of modes) is present.

Model	$\log B_{s,n}$	M_f/M_\odot	a_f
IMR (LVC)	-	$68.0^{+3.2}_{-3.0}$	$0.69^{0.05}_{0.04}$
DS - 1 mode	56.3	-	-
DS - 2 modes	55.4	-	-
Kerr - (2,2,0) mode	56.5	$64.6^{+14.3}_{-11.4}$	$0.50^{+0.28}_{-0.40}$
Kerr - (2,1,0) mode	56.6	$61.2^{+8.9}_{-8.5}$	$0.60^{+0.28}_{-0.49}$
Kerr - (2,0,0) mode	56.0	$55.0^{+4.1}_{-4.1}$	$0.69^{+0.27}_{-0.58}$
Kerr - (3,-3,0) mode	57.2	$72.3^{+9.7}_{-8.1}$	$0.46^{+0.47}_{-0.42}$
Kerr - (3,-2,0) mode	57.0	$75.7^{+7.1}_{-5.5}$	$0.49^{+0.44}_{-0.43}$
Kerr - (3,-1,0) mode	57.0	$79.9^{+4.5}_{-3.8}$	$0.47^{+0.46}_{-0.43}$
Kerr - (2,2,0),(3,-3,0) modes	56.7	$69.2^{+12.1}_{-14.2}$	$0.50^{+0.40}_{-0.44}$
Kerr - (2,2,0),(2,1,0) modes	56.2	$62.7^{+15.6}_{-9.9}$	$0.54^{+0.31}_{-0.44}$
Kerr - $\ell = 2$ modes	55.0	$55.1^{+15.5}_{-7.9}$	$0.53^{+0.54}_{-0.46}$
Kerr - $\ell = 3$ modes	54.3	$81.9^{+13.2}_{-10.5}$	$0.31^{+0.54}_{-0.28}$
Kerr - $\ell = 2, 3$ modes	52.0	$56.6^{+27.9}_{-10.1}$	$0.39^{+0.47}_{-0.36}$

vious studies. Bayesian model selection indicates that the data do not provide evidence in support of the presence of multiple QNM. We attempted to identify which QNM is actually dominant, obtaining the (3,-3,0), (3,-2,0), (2,1,0) and (2,2,0) modes as the most probable ones. At the GW150914 SNR, we cannot determine univocally the QNM label, in agreement with preliminary results on numerical relativity waveforms not presented here for brevity. More targeted investigations based on the Kerr BH solution, confirm our model-independent findings as well as our current lack of mode resolving power. We note that, due to the similar mode frequencies for the aforementioned subset of modes excited in a near-equal-mass BHs coalescence with weak spins, BH spectroscopy with a moderate SNR will require the use of information from the inspiral phase to determine the most likely of these modes. A systematic investigation of the details of our method applied to numerical waveforms, together with the inclusion of refined waveform models incorporating GR numerical predictions on the excitations and phases of the modes, will be presented in a future study. The analysis briefly presented in this *letter* can and will be applied to louder and/or multiple GW events. Joint coherent analyses will help to test the predictions of linearized GR. Such an extension of the present work will be presented in a future publication. We also defer to a further publication a detailed analysis (whose final null

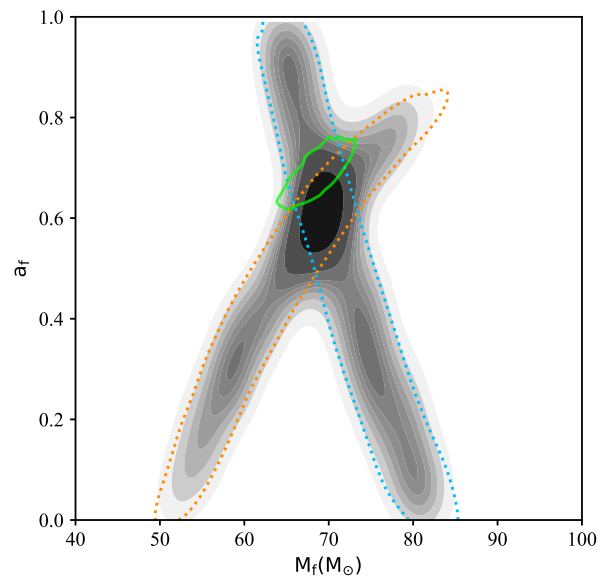


FIG. 3. Posterior distribution for M_f and a_f assuming the presence of individual modes: $(\ell, m, n) = (2, 2, 0)$ (dotted orange line) or $(\ell, m, n) = (3, -3, 0)$ (blue dotted line), and from a two-modes analysis $\{(2, 2, 0), (3, -3, 0)\}$ whose posterior density is represented in shades of gray. In green, the posterior for M_f and a_f from the LVC IMR analysis. The inferred mass and spin are consistent among the three cases considered, as well as with the LVC posteriors, in line with the Bayes factors, Table I, which indicate no preference towards any of them. See the text for a more in depth explanation.

result was anticipated in this paper) measuring relative deviations from GR ringdown frequencies [41, 49].

Acknowledgments The authors would like to thank Lionel London for providing a fit of the spheroidal harmonics. We are grateful to Abhirup Ghosh for useful discussions and to Vivien Raymond for suggestions on the manuscript. This work greatly benefited from discussions within the *strong-field* working group of the LIGO/Virgo collaboration. W.D.P. is funded by the “Rientro dei Cervelli Rita Levi Montalcini” Grant of the Italian MIUR. JV was supported by STFC grant ST/K005014/2. This work made use of the ARCCA Raven cluster, funded by STFC grant ST/I006285/1 supporting UK Involvement in the Operation of Advanced LIGO. This research has made use of data, software and/or web tools obtained from the Gravitational Wave Open Science Center (<https://www.gw-openscience.org>), a service of LIGO Laboratory, the LIGO Scientific Collaboration and the Virgo Collaboration. LIGO is funded by the U.S. National Science Foundation. Virgo is funded by the French Centre National de Recherche Scientifique (CNRS), the Italian Istituto Nazionale della Fisica Nucleare (INFN) and the Dutch Nikhef, with contributions by Polish and Hungarian institutes.

-
- [1] B. P. Abbott, R. Abbott, T. D. Abbott, M. R. Abernathy, F. Acernese, K. Ackley, C. Adams, T. Adams, P. Addesso, R. X. Adhikari, et al. (LIGO Scientific Collaboration and Virgo Collaboration), Phys. Rev. Lett. **116**, 061102 (2016), URL <https://link.aps.org/doi/10.1103/PhysRevLett.116.061102>.
- [2] C. V. Vishveshwara, Phys. Rev. D **1**, 2870 (1970), URL <https://link.aps.org/doi/10.1103/PhysRevD.1.2870>.
- [3] W. H. Press, Astrophys. J. **170**, L105 (1971).
- [4] S. Chandrasekhar and S. L. Detweiler, Proc. Roy. Soc. Lond. **A344**, 441 (1975).
- [5] R. H. Price, Phys. Rev. D **5**, 2439 (1972), URL <https://link.aps.org/doi/10.1103/PhysRevD.5.2439>.
- [6] V. Ginzburg and L. Ozernoy, Zh. Eksp. Teor. Fiz. **147**, 1030 (1964).
- [7] A. Doroshkevich, Y. B. Zeldovich, and I. Novikov, Sov. Phys. JETP **36** 1 (7) (1965).
- [8] W. Israel, Phys. Rev. **164**, 1776 (1967), URL <https://link.aps.org/doi/10.1103/PhysRev.164.1776>.
- [9] B. Carter, Phys. Rev. Lett. **26**, 331 (1971), URL <https://link.aps.org/doi/10.1103/PhysRevLett.26.331>.
- [10] S. W. Hawking, Communications in Mathematical Physics **25**, 152 (1972), ISSN 1432-0916, URL <https://doi.org/10.1007/BF01877517>.
- [11] D. C. Robinson, Phys. Rev. Lett. **34**, 905 (1975), URL <https://link.aps.org/doi/10.1103/PhysRevLett.34.905>.
- [12] P. O. Mazur, J. Phys. **A15**, 3173 (1982).
- [13] G. Bunting, Ph. D. Thesis (unpublished) University of New England, Armidale, N. S. W. (1983).
- [14] F. Pretorius, *Gravitational wave observation of dynamical, strong-field gravity*, Stephen Hawking 75th Birthday Conference on Gravity and Black Holes, DAMTP, Cambridge (2017).
- [15] M. Dafermos and I. Rodnianski, Clay Math. Proc. **17**, 97 (2013), 0811.0354.
- [16] V. Cardoso, E. Franzin, and P. Pani, Phys. Rev. Lett. **116**, 171101 (2016), URL <https://link.aps.org/doi/10.1103/PhysRevLett.116.171101>.
- [17] S. Hod, Phys. Rev. **D84**, 124030 (2011), 1112.3286.
- [18] G. Raposo, P. Pani, and R. Emparan (2018), 1812.07615.
- [19] O. Dreyer, B. J. Kelly, B. Krishnan, L. S. Finn, D. Garrison, and R. Lopez-Aleman, Class. Quant. Grav. **21**, 787 (2004), gr-qc/0309007.
- [20] E. Berti, V. Cardoso, and C. M. Will, Phys. Rev. **D73**, 064030 (2006), gr-qc/0512160.
- [21] H. Yang, K. Yagi, J. Blackman, L. Lehner, V. Paschalidis, F. Pretorius, and N. Yunes, Phys. Rev. Lett. **118**, 161101 (2017), 1701.05808.
- [22] R. Brito, A. Buonanno, and V. Raymond, Phys. Rev. **D98**, 084038 (2018), 1805.00293.
- [23] B. P. Abbott et al. (VIRGO, LIGO Scientific) (2013), [Living Rev. Rel.19,1(2016)], 1304.0670.
- [24] J. Aasi et al. (LIGO Scientific), Class. Quant. Grav. **32**, 074001 (2015), 1411.4547.
- [25] F. Acernese et al. (Virgo), Class. Quant. Grav. **32**, 024001 (2015), 1408.3978.
- [26] B. P. Abbott, R. Abbott, T. D. Abbott, M. R. Abernathy, F. Acernese, K. Ackley, C. Adams, T. Adams, P. Addesso, R. X. Adhikari, et al. (LIGO Scientific and Virgo Collaborations), Phys. Rev. Lett. **116**, 221101 (2016), URL <https://link.aps.org/doi/10.1103/PhysRevLett.116.221101>.
- [27] S. Bhagwat, M. Okounkova, S. W. Ballmer, D. A. Brown, M. Giesler, M. A. Scheel, and S. A. Teukolsky, Phys. Rev. **D97**, 104065 (2018), 1711.00926.
- [28] G. Carullo et al., Phys. Rev. **D98**, 104020 (2018), 1805.04760.
- [29] M. Cabero, C. D. Capano, O. Fischer-Birnholtz, B. Krishnan, A. B. Nielsen, A. H. Nitz, and C. M. Biwer, Phys. Rev. **D97**, 124069 (2018), 1711.09073.
- [30] R. P. Kerr, Phys. Rev. Lett. **11**, 237 (1963).
- [31] *The gravitational-wave open science center*, URL <https://www.gw-openscience.org/about/>.
- [32] M. Vallisneri, J. Kanner, R. Williams, A. Weinstein, and B. Stephens, J. Phys. Conf. Ser. **610**, 012021 (2015), 1410.4839.
- [33] W. Del Pozzo and J. Veitch, *CPNest: an efficient python parallelizable nested sampling algorithm*, <https://github.com/johnveitch/cpnest>.
- [34] L. London, D. Shoemaker, and J. Healy, Phys. Rev. D **90**, 124032 (2014), URL <https://link.aps.org/doi/10.1103/PhysRevD.90.124032>.
- [35] T. D. Abbott et al. (LIGO Scientific, Virgo), Phys. Rev. **X6**, 041014 (2016), 1606.01210.
- [36] W. G. Anderson, P. R. Brady, J. D. Creighton, and É. É. Flanagan, Phys. Rev. D **63**, 042003 (2001), gr-qc/0008066.
- [37] <https://dcc.ligo.org/LIGO-T1800235/public>.
- [38] X. Jiménez-Forteza, D. Keitel, S. Husa, M. Hannam, S. Khan, and M. Pürrer, Phys. Rev. D **95**, 064024 (2017), URL <https://link.aps.org/doi/10.1103/PhysRevD.95.064024>.
- [39] <https://pages.jh.edu/~eberti2/ringdown/>.
- [40] B. P. Abbott et al. (Virgo, LIGO Scientific), Phys. Rev. Lett. **116**, 241102 (2016), 1602.03840.
- [41] S. Gossan, J. Veitch, and B. S. Sathyaprakash, Phys. Rev. D **85**, 124056 (2012), URL <https://link.aps.org/doi/10.1103/PhysRevD.85.124056>.
- [42] E. Thrane, P. D. Lasky, and Y. Levin, Phys. Rev. **D96**, 102004 (2017), 1706.05152.
- [43] V. Baibhav, E. Berti, V. Cardoso, and G. Khanna, Phys. Rev. **D97**, 044048 (2018), 1710.02156.
- [44] E. Berti and A. Klein, Phys. Rev. **D90**, 064012 (2014), 1408.1860.
- [45] I. Kamaretsos, M. Hannam, S. Husa, and B. S. Sathyaprakash, Phys. Rev. D **85**, 024018 (2012), URL <https://link.aps.org/doi/10.1103/PhysRevD.85.024018>.
- [46] L. T. London (2018), 1801.08208.
- [47] A. Buonanno, L. E. Kidder, and L. Lehner, Phys. Rev. D **77**, 026004 (2008), URL <https://link.aps.org/doi/10.1103/PhysRevD.77.026004>.
- [48] J. G. Baker, W. D. Boggs, J. Centrella, B. J. Kelly, S. T. McWilliams, and J. R. van Meter (2008), arXiv:0805.1428.
- [49] J. Meidam, M. Agathos, C. Van Den Broeck, J. Veitch, and B. S. Sathyaprakash, Phys. Rev. D **90**, 064009 (2014), URL <https://link.aps.org/doi/10.1103/PhysRevD.90.064009>.